

Contributions of Vibronic Couplings to Photoelectron Spectroscopy in a Dimer: The Case of an Organic Mixed-Valence System

XianKai Chen*

Institute of Functional Nano and Soft Materials (FUNSOM), Joint International Research Laboratory of Carbon-Based Functional Materials and Devices, Soochow University, Suzhou, Jiangsu, 215123, People's Republic of China.

*Corresponding author: xkchen@suda.edu.cn

Received on 26 February 2025; Accepted on 29 March 2025

Abstract

In the framework of a dynamic vibronic model, we report the influence of both local and nonlocal vibronic coupling on the vibronic energy levels for organic mixed-valence systems, and then evaluate their contributions to photoelectron spectroscopy of a realistic molecule as an example. Our results demonstrate that the variation of nonlocal vibronic coupling constant in the dimeric model doesn't influence the relative positions of vibronic energy levels. For the spectrum simulated, it tries to maintain the constant difference $2t_{ab}^0$ between the splitting energy levels corresponding to two peaks of the first ionizations.

Key words: mixed-valence system, organic semiconductor, vibronic coupling, UPS.

The understanding of electron transfer (ET) process is of fundamental importance, which is the most active research area in chemistry, biology, and physics. ET is a dynamic process; the electronic motion accompanies a change of nuclear configuration, and the electronic and vibronic couplings (VC) are essential to the problem. However, in spite of extensive efforts, reaching a complete understanding of ET is still unsatisfying.

Organic mixed-valence (OMV) systems are of immense interest, since they are the simplest “dimeric” model compounds in studies on ET processes [1–7]. These compounds consist of only two charge-bearing “monomers” (M_a and M_b) which can be linked directly or via a bridging ligand BL . Many optoelectronic properties of OMV compounds are mainly determined by electronic coupling between the monomers and vibrational reorganization energies. This electronic coupling between the monomers is described by transfer integral

$$t_{ab} = \langle \varphi_a | \hat{H} | \varphi_b \rangle,$$

where \hat{H} is the molecular Hamiltonian, and two localized states φ_a and φ_b are corresponding to two valence structures $M_a - BL - M_b^+$ or $M_a^+ - BL - M_b$ in the absence of any coupling between the monomers. The reorganization energies are classified into the local intra-monomer (λ) and nonlocal inter-monomer (L) parts, which is similar with the case of organic crystals [8]. Electronic coupling and reorganization energies in OMV systems are usually

estimated by several experimental methods. According to Hush's semiclassical formalism [9], electronic coupling and reorganization energies can be predicted by analyzing the inter-valence charge-transfer (IVCT) band. Another experimental method widely applied to probe the electronic coupling is based on ET rate between the monomers measured by electron spin resonance (ESR) spectroscopy [10–12]. Electronic coupling can be also measured using gas-phase ultraviolet photoelectron spectroscopy (UPS) directly [13, 14]. Previous theoretical studies systematically investigated the effects of several important factors (such as electronic coupling, reorganization energies, and temperature) on IVCT bands of the typical OMV compounds by employing dynamic vibronic model combined with quantum chemical calculation [15–17]. Meantime, they also simulated their ESR spectra successfully [14]. Nevertheless, the contributions of vibronic coupling to UPS in OMV systems aren't still studied to date. Even in the polaron cluster model extensively studied [18, 19], the role of nonlocal VC in UPS remains unclear. Therefore, these points are our focus in this work.

In this Communication, to clarify the contributions of VC to UPS in OMV systems, their effects on vibronic energy levels of these molecules should be firstly discussed. Within localized φ_a and φ_b electronic bases, these systems are described by the following vibronic Hamiltonian:

$$\hat{H}_{\text{vib}} = \begin{pmatrix} g\hbar\omega_L(Q_+ + Q_-) & t_{ab}^0 + \sqrt{2}\alpha\hbar\omega_{NL}Q_{NL} \\ +\frac{\hbar\omega_L}{2}(P_+^2 + Q_+^2) & \\ +\frac{\hbar\omega_L}{2}(P_-^2 + Q_-^2) & \\ +\frac{\hbar\omega_{NL}}{2}(P_{NL}^2 + Q_{NL}^2) & \\ t_{ab}^0 + \sqrt{2}\alpha\hbar\omega_{NL}Q_{NL} & g\hbar\omega_L(Q_+ - Q_-) \\ & +\frac{\hbar\omega_L}{2}(P_+^2 + Q_+^2) \\ & +\frac{\hbar\omega_L}{2}(P_-^2 + Q_-^2) \\ & +\frac{\hbar\omega_{NL}}{2}(P_{NL}^2 + Q_{NL}^2) \end{pmatrix} \quad (1)$$

Here, P is nuclear momentum; Q_+ and Q_- are the symmetrized dimensionless coordinates of the intra-monomer vibration with the energy $\hbar\omega_L$; Q_{NL} is the dimensionless coordinate of the inter-monomer vibration with the energy $\hbar\omega_{NL}$; the dimensionless VC constants g (local) and α (nonlocal) are given by reorganization energies λ ($\lambda = g^2\hbar\omega_L$) and L ($L = \alpha^2\hbar\omega_{NL}$), respectively [8, 20]. t_{ab}^0 is the transfer integral at the equilibrium geometry.

The solutions of the vibronic Hamiltonian, Eq. (1), are numerically obtained by expanding its ν th eigenstate $\Psi_\nu(r; Q_+, Q_-, Q_{NL})$ in terms of a direct product basis of localized electronic states as well as three harmonic-oscillator eigenfunctions $\chi_m(Q_+)$, $\chi_n(Q_-)$ and $\chi_q(Q_{NL})$:

$$\begin{aligned} \Psi_\nu(r; Q_+, Q_-, Q_{NL}) \\ = \varphi_a \sum_{mnq} C_{a;mnq}^\nu \chi_m(Q_+) \chi_n(Q_-) \chi_q(Q_{NL}) \\ + \varphi_b \sum_{mnq} C_{b;mnq}^\nu \chi_m(Q_+) \chi_n(Q_-) \chi_q(Q_{NL}) \end{aligned} \quad (2)$$

where r is electronic coordinate. By setting the vibrational quanta numbers (m , n and q) in this expansion, the solutions of this dynamic vibronic problem could be obtained with any arbitrary accuracy. Therefore, Lanczos algorithm is employed to diagonalize vibronic Hamiltonian numerically, and the number of vibrational bases is set to $60 \times 60 \times 60$ in all cases here. Note that the harmonic oscillator approximation is only valid in the low energy regime around the equilibrium geometry, and, the higher the energy, the stronger the anharmonic effect, especially for the low-frequency modes. For example, for linear absorption and emission spectra, anharmonicities can lead to frequently observed asymmetries between absorption and emission spectra [21, 22].

To simplify the calculation of eigenenergies of the vibronic Hamiltonian matrix, the item

$$\frac{\hbar\omega_L}{2}(P_+^2 + Q_+^2) + g\hbar\omega_L Q_+$$

is dropped in the diagonal term because it can't influence the positions of eigenenergies relative to the lowest level. According to the previous study results on OMV systems [15, 16], effective inter-monomer vibrational energies are larger than the intra-monomer ones, which is different from the case of organic crystals. Thus, in the present work, the effects of VC on vibronic energy levels are studied in the case, $\gamma = \hbar\omega_{NL}/\hbar\omega_L = 20.1$ (see Figure 1). For comparison, another case, $\gamma = 1.1$, is also considered. To avoid

any artificial overlap of electronic, local vibrational, and nonlocal vibrational energy levels, the relevant ratio values such as γ and $\frac{t_{ab}^0}{\hbar\omega_{NL}}$ are set to fraction values. From Figures 1 (a) and (c), it can be found that when $g = 0.0$, the increase of nonlocal VC constant from 0.0 to 2.0 for different transfer integral values doesn't change the relative positions of vibronic energy levels. It is consistent with the two-site semiclassical picture. Actually, it is well-understood from the adiabatic potential energies related to the ionization of a dimer in Figure S1. When an excess charge is added into the dimer, two delocalized states appear

$$\Psi_\pm = \frac{1}{\sqrt{2}}(\varphi_a \pm \varphi_b)$$

with energies

$$E^\pm = \frac{\hbar\omega_L}{2}(Q_{NL} \pm \sqrt{2}\alpha)^2 - \alpha^2\hbar\omega_{NL} \pm t_{ab}^0$$

Obviously, due to the polaron effect of nonlocal VC, the increase of α value leads to the decrease in the bottom of the two vibronic energy surfaces for E^+ and E^- by the same quantity. Noted that the result obtained in our two-site case is not in agreement with the one obtained in many-sites case [20, 23].

It should be mentioned that the same conclusion is also obtained in another case $\gamma' = \hbar\omega_L/\hbar\omega_{NL} = 20.1$ corresponding to the case of organic crystals (like as pentacene). From Figure 1, it can be also found that the tuning roles of local and nonlocal VC in vibronic energy levels show a competitive relationship.

Noted that nonlocal VC tries to keep the constant difference value $\Delta E = E^+ - E^-$ between the splitting energy levels, that is, $2t_{ab}^0$. In spite of $t_{ab}^0 > \frac{\lambda'}{2}$ or $t_{ab}^0 < \frac{\lambda'}{2}$, the same trend can be still observed.

Here, it should be mentioned that the change of the adiabatic parameter ($t_{ab}^0/\hbar\alpha$) also doesn't affect this behavior.

Now, this methodology is applied to a realistic OMV molecule A as an example (see Figure 2). We focus on its vibronic photoionization transitions in order to understand the characteristics of its experimental UPS spectrum. The spectral intensity $I(E)$ of the transition from the initial state $\Psi_{i,m}$ with energy $E_{i,m}$ to the manifold (2) of final vibronic states $\Psi_{f,\nu}$ with energies $E_{f,\nu}$ is given in the framework of the Fermi golden rule:

$$I(E) = 2\pi \sum_\nu \sum_m P(E_{i,m}) \left| \langle \Psi_{i,m} | \hat{T} | \Psi_{f,\nu} \rangle \right|^2 \delta(E - (E_{f,\nu} - E_{i,m})) \quad (3)$$

\hat{T} is an operator describing the interaction between photo and electron; $P(E_{i,m})$ is the probability distribution of the initial state $\Psi_{i,m}$ occupied. To reproduce the experimental UPS spectrum, the parameters in Eq. (1) are taken from the correlative literatures. The energy $\hbar\omega_{NL}$ of the inter-monomer vibrational mode was set to 1050 cm^{-1} , a value that falls in the region of the C-N stretching in triarylamine molecules [24]. The energy $\hbar\omega_L$ of the intra-monomer vibrational mode has been taken as 500 cm^{-1} . This choice for the $\hbar\omega_L$ energy is justified by the fact that $\hbar\omega_L$ is an effective mode that accounts for the overall effect of the low energy solvent modes and of all the intramolecular modes coupled to the ET process. In previous studies, the selection of the above parameter values brought very consistent results with the experiments [16]. Due to much larger energies of these vibration modes than the room temperature $k_B T$ value ($\approx 200 \text{ cm}^{-1}$), only the transition from the ground state $\Psi_{i,0}$ of the neutral molecule

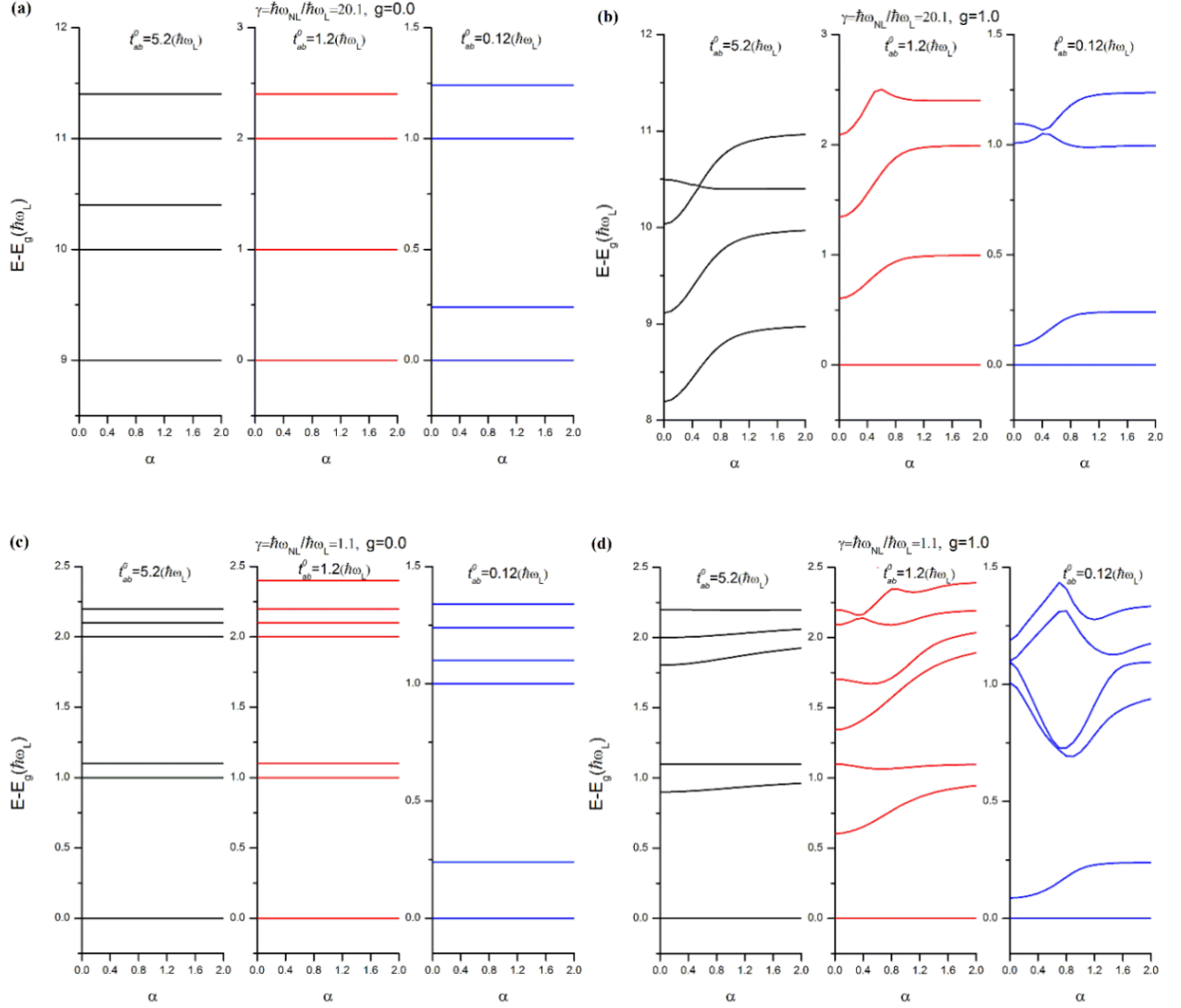


Figure 1. Change trends of the eigenenergies E relative to the lowest level E_g for different local and nonlocal vibronic coupling constants in two cases $\gamma = 20.1$ and $\gamma = 1.1$: (a) and (c) $g = 0.0$, (b) and (d) $g = 1.0$.

is taken into account in UPS spectrum. The VC constants and transfer integral are also obtained accordingly.

The spectrum simulated are given in Figure 2. The spectrum have been simulated assuming Gaussian line shape

$$\delta(E - (E_{f,\nu} - E_{i,m})) = \frac{1}{\Gamma\sqrt{\pi}} \exp(-[E - (E_{f,\nu} - E_{i,m})]^2 / \Gamma^2)$$

for each vibronic transition. Γ is set to be the same for all vibronic transitions. When the parameters are taken as $t_{ab}^0 = 2.0(\hbar\omega_L)$, $g = 2.24$, $\alpha = 0.87$ and $\gamma = 2.1$, our theoretical result is very close to the experimental UPS spectrum. For comparison, the case with only local or nonlocal VC is also shown in Figure 2. It can be found that both local and nonlocal VC can significantly reduce the intensity of spectrum, and simultaneously broaden the spectrum. We further analyze the respective roles of local and nonlocal VC in

UPS spectrum by tuning VC constants (see Figure S2). Regardless of local or nonlocal VC, the increase of coupling constants results in the shift of the photoionization peaks toward the high-energy region. As expected by us, the variation of nonlocal VC constant doesn't change the difference between the splitting energy levels corresponding to two peaks of the first ionizations in Figure S2(a), i.e. $\Delta E = E^+ - E^-$ is exactly equal to $2t_{ab}^0$. From Figure S2(b), our result supports the recent theoretical result obtained in optical absorption that the increase of local vibronic interaction should yield a smaller electronic coupling value if we try to reproduce the experimental spectrum [16]. When $t_{ab}^0/\hbar\omega_L < 1$ in Figure S2(c) and (d), the same conclusion is also obtained.

In summary, we employ a dynamic vibronic model to study the effects of VC on the vibronic energy levels in OMV systems, and then evaluate their contributions to UPS spectrum of a realistic

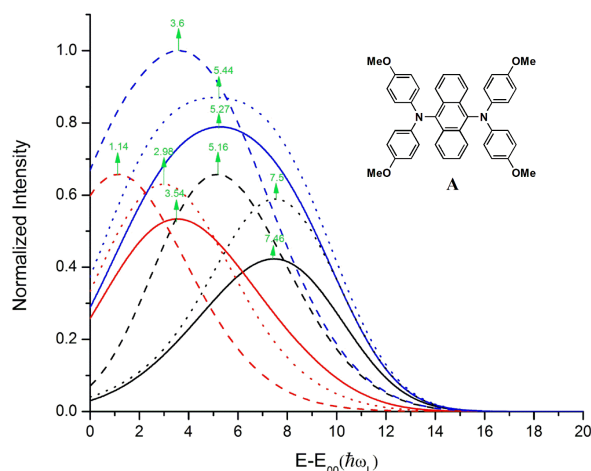


Figure 2. Calculated UPS spectrum profiles of the OMV molecule A for the following sets of parameters, $t_{ab}^0 = 2.0(\hbar\omega_L)$, $g = 2.24$, $\alpha = 0.87$ and $\gamma = 2.1$ (solid lines); $t_{ab}^0 = 2.0(\hbar\omega_L)$, $g = 0.0$, $\alpha = 0.87$ and $\gamma = 2.1$ (dashed lines); $t_{ab}^0 = 2.0(\hbar\omega_L)$, $g = 2.24$, $\alpha = 0.0$ and $\gamma = 2.1$ (dot lines). Red and black lines indicate the transition from the initial state $\Psi_{i,0}$ to the final delocalized state Ψ_- and Ψ_+ , respectively; Blue lines indicate the total photoelectron spectrum of the first ionizations. E_{00} is the transition energy from the ground state of the neutral molecule to the ground ionized state.

molecule taken as an example. Our results have indicated that the variation of nonlocal VC constant in the dimeric model doesn't influence the relative positions of vibronic energy levels. For UPS spectrum simulated, it tries to maintain the constant difference ($2t_{ab}^0$) between the splitting energy levels corresponding to two peaks of the first ionizations. Both local and nonlocal VC play very important role in broadening the UPS spectrum.

Supporting Information

The following supporting information can be downloaded at: <https://global-sci.com/storage/self-storage/cicc-2025-57-1-r1-si.pdf> Figure S1, Schematic diagram of the adiabatic potential energies related to the ionization of a dimer; Figure S2, Calculated UPS spectrum profiles for the following sets of parameters.

Acknowledgement

X.-K.C. gratefully acknowledges the financial support from the National Natural Science Foundation of China (Grant No. 52473190), the Natural Science Foundation of Jiangsu Province (Grant No. BK20240042), the Science and Technology Project of Suzhou (Grant No. ZX2024394), Suzhou Key Laboratory of Functional Nano & Soft Materials, Collaborative Innovation Center of Suzhou Nano Science & Technology, and the 111 Project.

References

[1] Barlow S., Risko C., Odom S. A., Zheng S., Coropceanu V., Beverina L., Brédas J.-L., Marder S. R. Tuning delocalization in the radical cations of 1,4-bis 4-(diarylamino)styryl benzenes,

2,5-bis 4-(diarylamino)styryl thiophenes, and 2,5-bis 4-(diarylamino)styryl pyrroles through substituent effects. *J. Am. Chem. Soc.*, **134** (2012), 10146.

[2] Lambert C., Noll G. One- and two-dimensional electron transfer processes in triarylamines with multiple redox centers. *Angew. Chem. Int. Ed.*, **37** (1998), 2107.

[3] Lambert C., Noll G. The class II/III transition in triarylamine redox systems. *J. Am. Chem. Soc.*, **121** (1999), 8434.

[4] Lambert C., Noll G., Schelter J. Bridge-mediated hopping or superexchange electron-transfer processes in bis(triarylamine) systems. *Nat. Mater.*, **1** (2002), 69.

[5] Nelsen S. F., Ismagilov R. F., Trieber D. A. Adiabatic electron transfer: Comparison of modified theory with experiment. *Science*, **278** (1997), 846.

[6] Nelsen S. F., Konradsson A. E., Weaver M. N., Telo J. P. Intervalence near-IR spectra of delocalized dinitroaromatic radical anions. *J. Am. Chem. Soc.*, **125** (2003), 12493.

[7] Nie H.-J., Chen X., Yao C.-J., Zhong Y.-W., Hutchison G. R., Yao J. Electronic coupling between two amine redox sites through the 5,5'-positions of metal-chelating 2,2'-bipyridines. *Chem.-Eur. J.*, **18** (2012), 14497.

[8] Coropceanu V., Cornil J., da Silva Filho D. A., Olivier Y., Silbey R., Brédas J.-L. Charge transport in organic semiconductors. *Chem. Rev.*, **107** (2007), 926.

[9] Hush N. S. Distance dependence of electron-transfer rates. *Coordin. Chem. Rev.*, **64** (1985), 135.

[10] Lancaster K., Odom S. A., Jones S. C., Thayumanavan S., Marder S. R., Brédas J.-L., Coropceanu V., Barlow S. Intramolecular electron-transfer rates in mixed-valence triarylamines: Measurement by variable-temperature ESR spectroscopy and comparison with optical data. *J. Am. Chem. Soc.*, **131** (2009), 1717.

[11] Nelsen S. F., Ismagilov R. F., Powell D. R. Charge localization in a dihydrazine analogue of tetramethyl-*p*-phenylenediamine radical cation. *J. Am. Chem. Soc.*, **118** (1996), 6313.

[12] Nelsen S. F., Ismagilov R. F., Powell D. R. Charge-localized *p*-phenylenedihydrazine radical cations: ESR and optical studies of intramolecular electron transfer rates. *J. Am. Chem. Soc.*, **119** (1997), 10213.

[13] Coropceanu V., Gruhn N. E., Barlow S., Lambert C., Durivage J. C., Bill T. G., Noll G., Marder S. R., Brédas J. L. Electronic couplings in organic mixed-valence compounds: The contribution of photoelectron spectroscopy. *J. Am. Chem. Soc.*, **126** (2004), 2727.

[14] Lambert C., Risko C., Coropceanu V., Schelter J., Amthor S., Gruhn N. E., Durivage J. C., Brédas J. L. Electronic coupling in tetraanisylarylenediamine mixed-valence systems: The interplay between bridge energy and geometric factors. *J. Am. Chem. Soc.*, **127** (2005), 8508.

[15] Coropceanu V., Lambert C., Noll G., Brédas J. L. Charge-transfer transitions in triarylamine mixed-valence systems: The effect of temperature. *Chem. Phys. Lett.*, **373** (2003), 153.

[16] Coropceanu V., Malagoli M., André J. M., Brédas J. L. Charge-transfer transitions in triarylamine mixed-valence systems: A joint density functional theory and vibronic coupling study. *J. Am. Chem. Soc.*, **124** (2002), 10519.

[17] Coropceanu V., Malagoli M., André J. M., Brédas J. L. Intervalence transition in triarylamine mixed-valence systems: A time-dependent density functional theory study. *J. Chem. Phys.*, **115** (2001), 10409.

[18] Marsiglio F. The spectral-function of a one-dimensional Holstein polaron. *Phys. Lett. A*, **180** (1993), 280.

[19] Alexandrov A. S., Kabanov V. V., Ray D. K. From electron to small polaron: An exact cluster solution. *Phys. Rev. B*, **49** (1994), 9915.

[20] Li Y., Yi Y., Coropceanu V., Brédas J.-L. Symmetry effects on nonlocal electron-phonon coupling in organic semiconductors.

- Phys. Rev. B*, **85** (2012), 245201.
- [21] Wang Y., Ren J., Shuai Z. Evaluating the anharmonicity contributions to the molecular excited state internal conversion rates with finite temperature TD-DMRG. *J. Chem. Phys.*, **154** (2021), 214109
- [22] Pour A. G., Lincoln C. N., Perlík V., Šanda F., Hauer J. Anharmonic vibrational effects in linear and two-dimensional electronic spectra. *Phys. Chem. Chem. Phys.*, **19** (2017), 24752.
- [23] Fratini S., Ciuchi S. Bandlike motion and mobility saturation in organic molecular semiconductors. *Phys. Rev. Lett.*, **103** (2009), 266601.
- [24] Pacansky J., Waltman R. J., Seki H. *Ab initio* computational studies on the structures and energetics of hole transport molecules: Triphenylamine. *B. Chem. Soc. Jpn.*, **70** (1997), 55.